

Efficient exploration of energy landscapes

Martin Mann

Bioinformatics Group, University of Freiburg, Georges-Köhler-Allee 106, D-79110 Freiburg, Germany

Konstantin Klemm

Bioinformatics Group, University of Leipzig, Härtelstrasse 16-18, D-04107 Leipzig, Germany

Abstract. Many physical and chemical processes, such as folding of biopolymers, are best described as dynamics on large combinatorial energy landscapes. A concise approximate description of dynamics is obtained by partitioning the micro-states of the landscape into macro-states. Since most landscapes of interest are not tractable analytically, the probabilities of transitions between macro-states need to be extracted numerically from the microscopic ones, typically by full enumeration of the state space. Here we propose to approximate transition probabilities by a Markov chain Monte-Carlo method. For landscapes of the number partitioning problem and an RNA switch molecule we show that the method allows for accurate probability estimates with significantly reduced computational cost.

PACS numbers: 05.10.Ln, 87.15.H-, 02.50.Ga

1. Introduction

Energy landscapes [1] are a key concept for the description of complex physical and biological systems. In particular, the dynamics of structure formation (“folding”) of biopolymers, e.g. protein or ribonucleic acids, can be understood in terms of their energy landscapes [2]. Formally, a landscape is determined by a set X of micro-states (or conformations), a neighborhood structure of X that encodes which conformations can be reached from which other ones, and an energy function $E : X \rightarrow \mathbb{R}$ which assigns an energy value to each state. In the case of ribonucleic acids it has been demonstrated that the dynamics of the folding process can be captured in good approximation by merging large contiguous sets of micro-states into macro-states [3]. A typical mapping is in terms of gradient basins, where each local energy minimum and its gradient basin form a macro-state.

Given such a partitioning of the landscape, the dynamics is approximately described as a Markov chain on the set of macro-states. In order to obtain this description, the transition probabilities between macro-states in this Markov chain need to be extracted from the original energy landscape.

Existing approaches [4, 5, 6, 7] for *transition rate estimation* are based on enumeration of all micro-states. For landscapes of real combinatorial problems or long biopolymers with billions of micro-states, however, enumeration is impractical with the given time resources. Typically, limited storage capacity puts even more severe restrictions on the size of tractable problems because a large fraction of the enumerated micro-states needs to be kept in working memory. Wolfinger et al. [7] partially circumvent this problem by considering only the low-energy fraction of the landscape that is tractable with the available resources.

Here we suggest a Markov chain Monte-Carlo sampling method for transition matrix estimation. At difference with the earlier approaches, the memory requirement scales only with the number of non-zero transition probabilities to be determined. Other recent methods of stochastic landscape exploration [8, 9] use trajectories of the original dynamics for counting transitions between macro-states. In contrast, the idea behind the present method is to explicitly explore boundaries between macro-states. To this end, we confine the dynamics into a single macro-state b and find and count possible transitions from b to all adjacent macro-states. This strategy allows to select the regions of the landscape to be explored and the precision to be applied.

2. Landscape and micro-state dynamics

As mentioned in the introduction, an energy landscape is a triple (X, E, M) where

- X is a finite set of states,
- $E : X \rightarrow \mathbb{R}$ is an energy function on X , and
- $M : X \rightarrow \mathcal{P}(X)$ is a neighborhood function or “move set” that assigns to each state $x \in X$ the set of its directly accessible neighbouring states. $\mathcal{P}(X)$ is the power set

of X . Here we assume that M is symmetric, *i.e.* $x \in M(y) \Rightarrow y \in M(x)$. By Δ we denote the maximum number of neighbours, $\Delta = \max_{x \in X} |M(x)|$.

We consider a time-discrete stochastic dynamics on the state set X . Having the Markov property, the dynamics is defined by giving the transition probability $p_{x \rightarrow y}$ from each $x \in X$ to each $y \in M(x)$. Provided the system is in state x at time t , $p_{x \rightarrow y}$ is the probability that the system is in state y at time $t + 1$. With probability $p_{x \rightarrow x} = 1 - \sum_{y \in M(x)} p_{x \rightarrow y}$, the system remains at state x .

Specifically, the Metropolis probabilities at inverse temperature β ,

$$p_{x \rightarrow y} = \Delta^{-1} \min\{\exp(\beta[E(x) - E(y)]), 1\} \quad (1)$$

are used throughout this contribution. This choice, however, is not compulsory. All that follows, and in particular the estimation by sampling, applies to arbitrary choices of transition probabilities leading to *ergodic* Markov chains. The ergodicity is important because we need a unique stationary distribution $P(x)$ on X .

3. Partitioning and macro-state dynamics

A partitioning of the landscape is a mapping F from the set of micro-states X into a set of macro-states B . Our goal here is to find a dynamics on B that does have the Markov property while following the original micro-state dynamics as closely as possible. In general, however, a Markov chain is not obtained as the direct mapping $(F(x_t))_{t=0}^\infty$ of a Markov chain $(x_t)_{t=0}^\infty$ generated by the dynamics on X . The reason can be sketched as follows. When the system is in a macro-state $b \in B$, the probability of exiting to a macro-state c depends on where exactly (in which micro-state) the system is inside b . The micro-state assumed inside b , however, depends on how the system entered b , which is again influenced by the macro-state a assumed before entering b .

Thus, we make the following simplifying assumption. Given that the system is found in macro-state $b \in B$, the micro-state $x \in X$ is distributed as

$$P_b(x) = \begin{cases} P(x) / \sum_{y \in F^{-1}(b)} P(y) & \text{if } x \in F^{-1}(b) \\ 0 & \text{otherwise} \end{cases} \quad (2)$$

This is the stationary distribution P of the whole system restricted to micro-states in b and normalized appropriately. Under this assumption, the probability of a transition to macro-state c , when being in macro-state $b \neq c$ is

$$q_{b \rightarrow c} = \sum_{x \in F^{-1}(b)} \left(P_b(x) \sum_{y \in M(x) \cap F^{-1}(c)} p_{x \rightarrow y} \right) \quad (3)$$

The inner sum is the probability of going to a micro-state y belonging to macro-state c and being a neighbour of x , given that the system is in state x . The outer sum represents the equilibrium weighting of the micro-states x inside the given macro-state b . A straight-forward method determines the exact transition probabilities by performing

the sums in Eq. (3), *i.e.* exhaustive enumeration of all micro-states and all neighbours [6, 7].

Throughout this contribution, we consider a partitioning of X with respect to gradient basins. Two micro-states $x, y \in X$ lie in the same macro-state $F(x) = F(y)$ if and only if the steepest descent walks starting in x and y terminate in the same local minimum. A state $u \in X$ is called local minimum, if $E(v) > E(u)$ for all $v \in M(u)$. In order for the steepest descent to be well-defined, each state $x \in X$ that is not a local minimum must have a unique neighbour $y \in M(x)$ with lowest energy. If this is not the case, the ambiguity is resolved by further criteria, see also Appendix B. For a given landscape and partitioning, the macro-state transition probabilities can be estimated by the sampling algorithm presented in the next section.

4. Sampling method

The method we introduce computes an estimate of the transition probabilities q in Equation (3) by a standard importance sampling restricted to a macro-state b using the micro-state probabilities $P_b(x)$ defined in Equation (2). Being in state $x_t \in F^{-1}(b)$ at time t , a neighbour $z \in M(x_t)$ is drawn at random with equal probabilities. The suggestion is accepted as the next state, $x_{t+1} = z$, with probability $\min\{1, P_b(y)/P_b(x_t)\}$. Otherwise the state remains the same, $x_{t+1} = x_t$. This choice guarantees that the relative frequency of state x tends towards the relative frequency $P_b(x)$ for increasing chain length $t \rightarrow \infty$ [10]. For a realization of a Markov chain of length t_{\max} , transition probabilities are estimated as

$$q'_{b \rightarrow c} = \frac{1}{t_{\max}} \sum_{t=1}^{t_{\max}} \sum_{y \in M(x_t) \cap F^{-1}(c)} p_{x_t \rightarrow y} . \quad (4)$$

In practice, the inner summation is performed only once at each time t , because each neighbour y of x_t contributes to the transition probability to exactly one macro-state $F(y)$.

Computation time is saved by storing all visited micro-states of basin b and their sets of neighbours with transition probabilities in a data structure with fast search access, *e.g.* in a hash table. This is particularly advantageous in cases with broadly distributed micro-state probabilities such as Boltzmann weights at low temperature. Here the Markov chain will encounter the highly probable (low energy) micro-states many times but neighbour sets and transition probabilities are computed only once per state. In the usual cases where macro-states are defined as basins of local minima, memory of visited states also saves time in evaluating the macro-state assignment function F : When the gradient walk starting at state x reaches a micro-state known to be in basin b , x itself is known to belong to b . Thus in many cases the walk may be terminated before reaching the ground state.

So far we have described how to estimate probabilities of transitions from *one* macro-state b to others. By applying this procedure separately to each macro-state, the

full transition matrix q is obtained. This can be implemented as an iterative exploration of the energy landscape without initial knowledge of the set of macro-states. Whenever a neighbour y of a state x in the Markov chain belongs to a macro-state $F(y)$ not previously seen, we add the pair $(F(y), y)$ to a queue Q of macro-states yet to work on. Initially, Q may contain only one particular pair (b, x_0) , *e.g.* the completely unfolded state x_0 of a polymer and the corresponding macro-state $b = F(x_0)$. The iterative exploration of the landscape is implemented in the following loop. (i) Extract a pair (b, x_0) from Q ; (ii) generate Markov chain inside b , starting at x_0 ; (iii) obtain estimates according to Eq. (4) and add newly discovered macro-states to Q ; (iv) If Q is not empty, resume at (i). Note, this method is directly parallelizable and will easily profit from distributed computing. Here, several independent realizations of Markov chains with respect to different macro-states can be run simultaneously, extracting from and feeding to the same queue.

An implementation of the method is included in the Energy Landscape Library [11], version 3.2. ‡.

5. Results

We first test the method on the number partitioning landscape. Micro-states are configurations of N spins, $X = \{+1; -1\}^N$. Spin interactions involve frustration similar to spin-glasses. Appendix A gives the exact definition of the landscapes under consideration. The artificial number partitioning landscapes are particularly suitable for analysis of the system-size dependence of the sampling performance. Figure 1 shows the convergence of the probability estimates. For each system size N , the sampling error decreases inversely proportional to the number of sampling steps performed per basin. Error measurement utilizes the KL divergence from Appendix C. Larger systems need more computational effort to reach a certain precision. The inset of Fig. 1 indicates that the total computational effort required for the error to fall below a given value grows sub-exponentially with N , to be compared with a number of micro-states increasing as 2^N . Thus under growing N , sampling a strongly decreasing fraction of micro-states is sufficient in order to reach a given precision.

Let us now consider an RNA secondary structure folding landscape as a real-world application. Multistable RNAs, so called RNA-switches, are essential for the regulation of cellular processes. Thus, an understanding of the folding kinetics of such molecules is of high importance. For a detailed overview see [12]. Here, we investigate the bistable RNA d33 and its energy landscape introduced in Appendix B.

Figure 2 summarizes the evolution of the sampling error for increasing sampling steps per basin. As in the number partitioning landscape, KL decreases inversely proportional to the number of sampling steps. The mean of the distribution of KL values across basins is larger than the median by a factor of 3 indicating a broad distribution.

‡ note = Freely available at <http://www.bioinf.uni-freiburg.de/Software/>

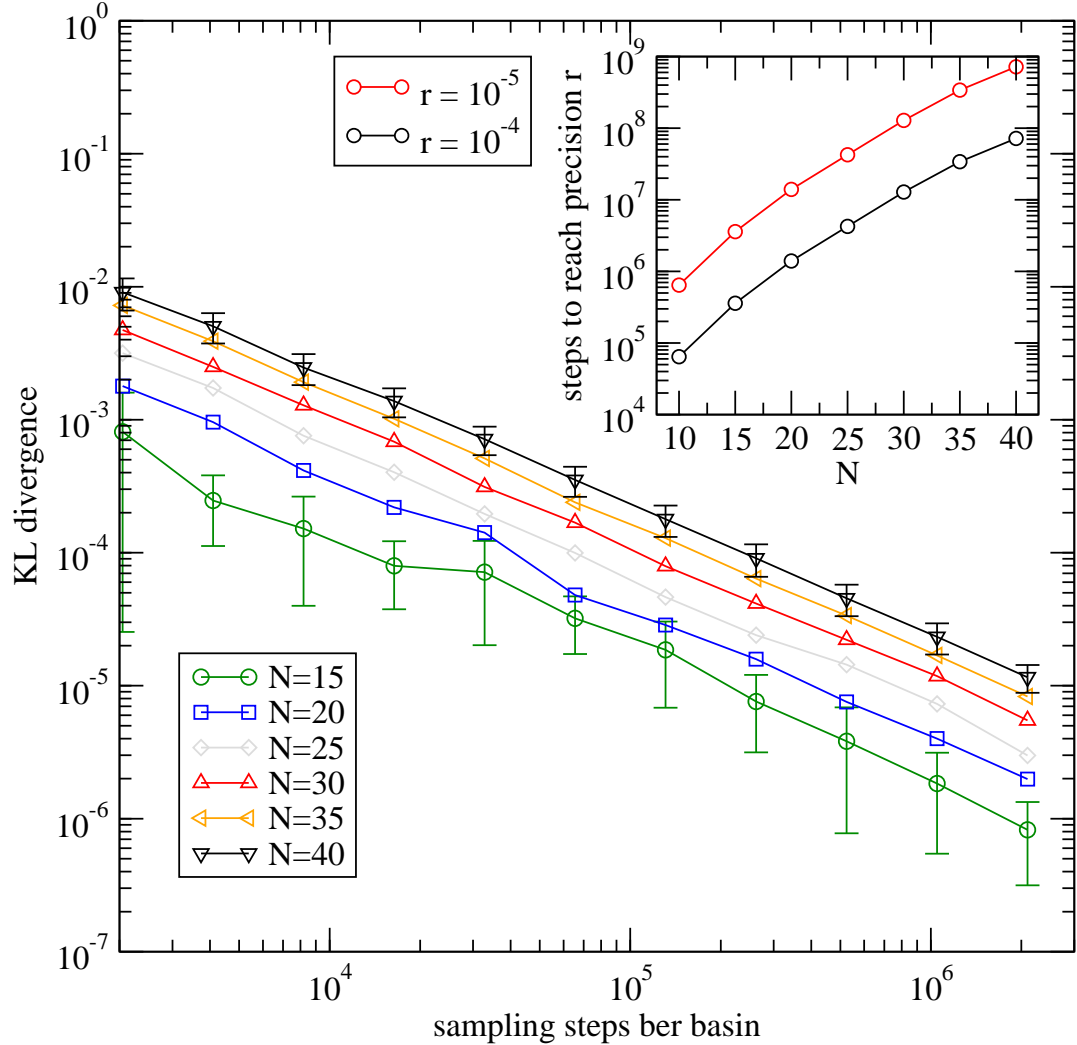


Figure 1. The deviation of estimated transition probabilities from the exact values is inversely proportional to the number of sampling steps (main panel). The analyzed landscapes are the special instances of number partitioning (Appendix A) for various sizes N . Error bars ($N = 15$ and $N = 40$) indicate the standard deviation between KL for different basins. The inset shows the N -dependence of the total number of sampling steps required for reaching a given precision, *i.e.* lowering KL divergence below r .

This is due to a broad distribution of macro-state sizes. Probability vectors for macro-states comprising one or a few micro-states reach a low error after fewer sampling steps than those for large macro-states. One of the extensions of the method outlined in section 6 chooses a number of sampling steps individually for each macro-state based on its estimated partition function.

In Figure 3, we compare the kinetics of the molecule for the approximated transition probabilities via sampling and the exact ones derived by the enumeration of the whole landscape. Already after 10^5 sampling steps per basin, no clear discrepancy between approximated and exact kinetics is observable (note concentration scale is logarithmic).

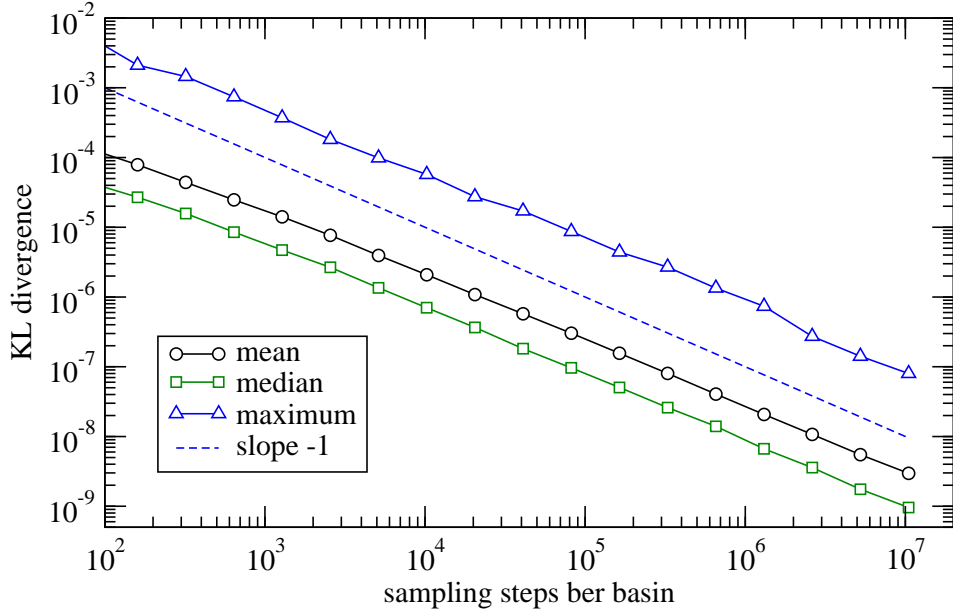


Figure 2. Time evolution of the sampling error (KL divergence) for the folding landscape of an RNA molecule (d33 - Appendix B). Mean, median, and maximum are for the distribution of KL values over the $|B| = 3223$ macro-states (local minima).

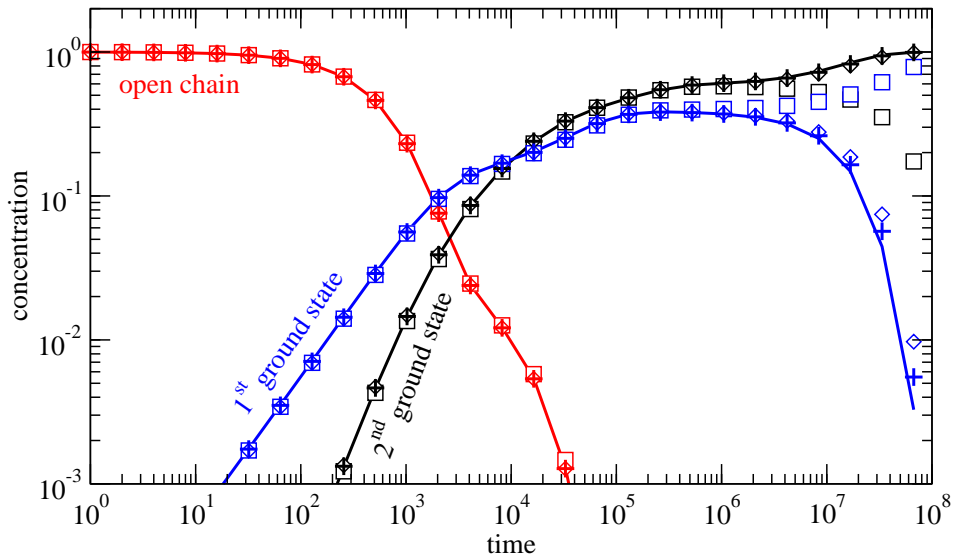


Figure 3. Time evolution of macro-state concentrations for RNA d33 from the exact transition probabilities (curves) and from approximated ones via sampling for 10^4 , 10^5 , and 10^6 steps per macro-state (squares, diamonds, and crosses).

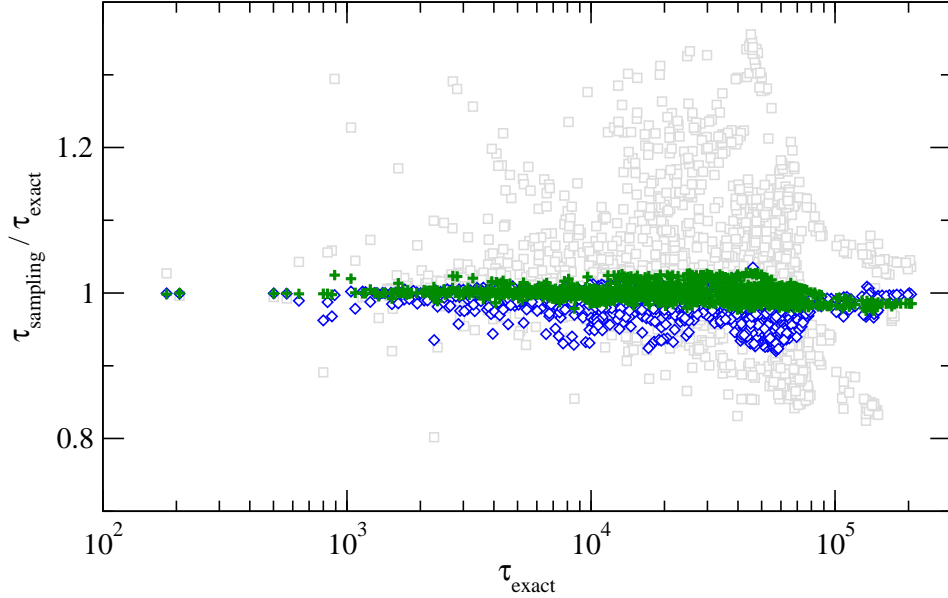


Figure 4. Sampling precision in terms of the predicted average time $\tau(b)$ to reach the ground state from a macro-state b . For each b , the corresponding data point gives the ratio between τ_{sampling} based on the sampled matrix and the value τ_{exact} from the exact matrix *versus* τ_{exact} itself. As in Figure 3, symbols distinguish number of sampling steps 10^4 (squares), 10^5 (diamonds), and 10^6 (crosses). The considered landscape is for RNA d-33. The target contains both ground states b_0 and b_1 , so $\tau(b_0) = \tau(b_1) = 0$. See Appendix C for details.

Since we hash the probabilities for already visited structures, the real time consumption per basin scales with the number of visited states instead of overall sampling steps. Thus, small basins are sampled much faster than larger ones. Therefore, our method is much faster than the exact but exhaustive enumeration approach. For instance, sampling with 10^5 steps per basin is 9 times faster than enumeration for d33 while still allowing for high accuracy. For 10^6 steps, still a speedup of 2.6 is observed. We discuss an extension of the method that will exploit the high variation of basin sizes to further speed up the method in Section 6.

Another comparison between exact and sampled transition probabilities is made in terms of the average time $\tau(b)$ from macro-state b to one of the ground states. For a biopolymer as considered here, $\tau(b)$ is the folding time when starting in an initial state b such as the open chain. See Appendix C for details. Figure 4 shows that $\tau(b)$ -values based on the sampled transition probabilities have small relative error for all starting macro-states $b \in B$. Already for 10^4 sampling steps per basin, the ratios between exact and approximate times τ are in the range $[0.8; 1.35]$. They fall into $[0.97; 1.03]$ when using 10^6 steps per basin.

6. Extensions and modifications of the method

In this section we list ideas for varying the method to potentially increase efficiency and applicability in various settings. We emphasize that these variations are not employed in the applications in section 5.

The stopping criterion (iv) of the outer loop (Sec. 4) may be modified if we do not aim to explore the whole landscape but only a subset of the set of macro-states. Then Q may be handled as a priority queue. For instance, we may be interested only in transitions between macro-states below a certain energy threshold or those involved in typical trajectories. In the latter case, the next macro-state to be explored is the one that is reached from already explored macro-states with the largest probability.

In addition to transition probabilities, the partition function

$$Z_b = \sum_{x \in F^{-1}(b)} \exp(-\beta E(x)) \quad (5)$$

of the macro-state b may be estimated at any time during the sampling. A lower bound on Z_b is obtained by restricting the summation in Eq. (5) to states $X(t) = \{x_s \mid s = 1, \dots, t\}$ encountered up to time t . This can be improved by using the estimated time that the Markov chain spends in states $X(t)$,

$$r(t) = \frac{|\{t < s \leq (t + \Delta t) \mid x_s \in X(t)\}|}{\Delta t} \quad (6)$$

with a suitably chosen Δt , *e.g.* $\Delta t = t$. Then

$$Z'_b(t) = \frac{1}{r(t)} \sum_{x \in X(t)} \exp(-\beta E(x)) \quad (7)$$

is an unbiased estimate of the partition function Z_b since $X(t) \subseteq F^{-1}(b)$. Furthermore, the estimate $r(t)$ may also be used for adapting the length of the Markov chain exploring macro-state b to the size of b . The sampling will be run until the fraction of covered probability mass exceeds a certain threshold, *e.g.* stopping as soon as $r(t) > 0.5$.

If the micro-state dynamics in terms of the transition probabilities $p_{x \rightarrow y}$ fulfills detailed balance, then so does the macro-state dynamics with transition probabilities $q_{b \rightarrow c}$ defined in Equation 3. Detailed balance means

$$Z_l q_{l \rightarrow s} = Z_s q_{s \rightarrow l} . \quad (8)$$

This knowledge may be used to check the quality of the estimates q' . One may also correct false zeros, *i.e.* transitions that were missed by the sampling but are known to exist because the reverse transition has been found.

7. Conclusion and discussion

When coarse-graining the state space of an energy landscape into macro-states, transition probabilities between macro-states have to be obtained in order to capture the coarse-grained stochastic dynamics. Here we have introduced a sampling method

that allows for fast yet accurate estimation of these transition probabilities. We have demonstrated the scalability of the approach with system size for special instances of the number partitioning problem. As an example of a real-world application, we have analyzed the folding landscape of the secondary structure of a biopolymer, in this case an RNA switch. Its rich dynamic behaviour is accurately rendered by transition probabilities obtained with low computational cost.

The general method as described and applied here may serve as a flexible framework for stochastic exploration of energy landscapes. We have sketched several extensions and modifications to obtain increased performance and wider applicability.

In ongoing and future work, the method shall be applied to other energy landscapes including those of state-discrete protein folding dynamics [13, 14]. Such landscapes have been shown to be amenable to sampling approaches [15]. Another field of application of our method is the clarification of concepts for dynamics on energy surfaces, such as the notion of a funnel [16, 17].

Acknowledgements

KK gratefully acknowledges funding from VolkswagenStiftung.

Appendix A. Number partitioning landscape

The number partitioning problem (NPP) is a decision problem in the theory of computation and computational complexity [18, 19, 20]. It asks if a given set A of N real non-negative numbers can be partitioned into two subsets B, C such that numbers in B have the same sum as those in C . In an equivalent formulation, we label the numbers in A as a_1, \dots, a_N and use spin variables x_1, \dots, x_N to encode if a_i is in subset B ($x_i = +1$) or in subset C ($x_i = -1$). This system has the set of micro-states $X = \{-1, +1\}^N$. We define the energy of state $x \in X$ as

$$E(x) = \left| \sum_{i=1}^N x_i a_i \right|. \quad (\text{A.1})$$

Then the NPP amounts to the question if the ground state energy of this system is zero.

The number partitioning *landscape* is obtained by using the hypercube as the neighborhood structure. For each $x \in X$ we have

$$M(x) = \{y \in X \mid d(x, y) = 1\} \quad (\text{A.2})$$

as the set of neighbours. The usual Hamming distance d is used, so $d(x, y)$ is the number of entries i such that $x_i \neq y_i$. A local move on the landscape means flipping one of the N spin variables x_i .

Random instances are typically generated by drawing the a_i as statistically independent random variables uniformly distributed in the unit interval. Then the expected number of local minima grows exponentially with N , more precisely $\langle |B| \rangle \sim 2^N N^{-3/2}$ [21].

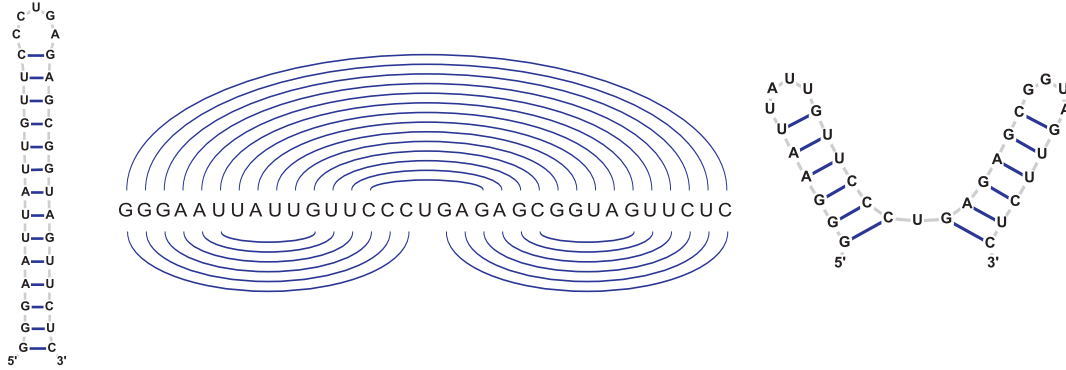


Figure B1. RNA secondary structures (left/right) with energies $-14.4 \frac{kcal}{mol}$ and $-14.3 \frac{kcal}{mol}$ of the tested bistable RNA d33 and their outer-planar linear Feynman diagrams (middle) (drawn using jViz.Rna v1.77 [23]). Energy evaluation and sequence design is based on Vienna RNA package v1.8.2 [24] and the method from [12].

Here we use special instances of the NPP where

$$a_i = (i - 1)^{-\alpha} \quad (\text{A.3})$$

with $\alpha = 0.55$. For these instances, we have found the number of local minima to grow exponentially with N for $N \leq 40$. However, the growth is much slower than for randomly generated instances. At $N = 40$, the instance of Equation (A.3) has 318 local minima, to be compared with an expected number of $\approx 10^{15}$ local minima for randomly generated instances.

Appendix B. RNA folding landscapes

As an example of folding landscapes of biopolymers we consider RNA molecules [22]. The primary structure of an RNA molecule is a finite sequence (a string) over the alphabet of the four nuclear bases $\{A, C, G, U\}$. An RNA secondary structure is a list of pairs (i, j) of positions in the primary structure such that the following conditions hold. (1) Base combinations at pairing positions must be **A-U** or **G-C** (Watson-Crick pairs) or **G-U** (wobble pair); (2) each position i can pair with at most one other position j ; (3) there are no two pairs (i, j) and (k, l) with $i < k < j < l$. The latter condition forbids so-called pseudoknots and makes the graph representation of a secondary structure outer-planar (see Fig. B1).

In the folding landscape of an RNA sequence, the set of micro-states X contains the valid secondary structures. The energy $E(x)$ of a secondary structure $x \in X$ is a sum over binding energies of stacks (contiguous regions of binding) and entropic contributions from open (unbound) sections of the RNA chain. For details of energy calculations, we refer to the literature [24, 25, 26]. Micro-states $x, y \in X$ are adjacent, *i.e.* $y \in M(x)$ and $x \in M(y)$, if y can be generated from x by adding or removing a single base pair. Shift moves [22] are not considered in this contribution. When the lowest energy neighbour

of a structure is not unique the degeneracy is resolved by an additional lexicographic ordering on string representations of the structures, see references [3, 7, 22] for details.

Specifically, we work with the bistable RNA d33 sequence shown in Fig. B1. It has 29,759,371 micro-states allowing for full enumeration. Out of the 3,223 local minima, the two lowest are the secondary structures given in Fig. B1. These two ground states have practically the same energy. They are separated by a large energy barrier, since a walk between them involves breaking all base pairs.

Appendix C. Error measure and time to target

The sampling error is measured by comparing, separately for each macro-state b , the exact and estimated transition probability vectors for leaving b . We quantify the discrepancy between the two vectors by the Kullback-Leibler divergence [27]

$$D(q'_b || q_b) = \sum_{c \in B} q'_{b \rightarrow c} \ln \frac{q'_{b \rightarrow c}}{q_{b \rightarrow c}} . \quad (\text{C.1})$$

For the number partitioning landscapes (Appendix A), the exact probability vector q_b is not available for comparison because the landscapes with up to 2^{40} states cannot be enumerated. Here we compare q'_b obtained after t_{\max} steps with the estimate after $2t_{\max}$ steps.

Given a set of target states $A \subset B$, the time to target is $\tau(a) = 0$ when starting in one of the target states $a \in A$ (boundary condition). For a starting state $b \in B \setminus A$, the average time $\tau(b)$ until first reaching one of the target states obeys the recursion

$$\tau(b) = 1 + \sum_{c \in B} q_{b \rightarrow c} \tau(c) . \quad (\text{C.2})$$

References

- [1] Christian M. Reidys and Peter F. Stadler. Combinatorial landscapes. *SIAM Rev.*, 44(1):3–54, 2002.
- [2] C. B. Anfinsen. Principles that govern the folding of protein chains. *Science*, 181:223–230, 1973.
- [3] Michael T. Wolfinger, W. Andreas Svrcek-Seiler, Christoph Flamm, Ivo L. Hofacker, and Peter F. Stadler. Exact folding dynamics of RNA secondary structures. *J. Phys. A: Math. Gen.*, 37:4731–4741, 2004.
- [4] Hue Sun Chan and Ken A. Dill. Transition states and folding dynamics of proteins and heteropolymers. *The Journal of Chemical Physics*, 100(12):9238–9257, 1994.
- [5] S. Wuchty, W. Fontana, I. L. Hofacker, and P. Schuster. Complete suboptimal folding of RNA and the stability of secondary structures. *Biopolymers*, 49:145–165, 1999.
- [6] Paolo Sibani, Ruud van der Pas, and J. Christian Schön. The lid method for exhaustive exploration of metastable states of complex systems. *Computer Physics Communications*, 116(1):17–27, 1999.
- [7] Michael T. Wolfinger, Sebastian Will, Ivo L. Hofacker, Rolf Backofen, and Peter F. Stadler. Exploring the lower part of discrete polymer model energy landscapes. *Europhys. Lett.*, 74:726–732, 2006.
- [8] D. Gfeller, P. De Los Rios, A. Caflisch, and F. Rao. Complex network analysis of free-energy landscapes. *Proceedings of the National Academy of Sciences*, 104(6):1817–1822, 2007.

- [9] Diego Prada-Gracia, Jesús Gómez-Gardeñes, Pablo Echenique, and Fernando Falo. Exploring the free energy landscape: From dynamics to networks and back. *PLoS Comput Biol*, 5(6):e1000415, 2009.
- [10] Nicholas Metropolis, Arianna W. Rosenbluth, Marshall N. Rosenbluth, and Augusta H. Teller. Equation of state calculations by fast computing machines. *J. Chem. Phys.*, 21:1087–1092, 1953.
- [11] Martin Mann, Sebastian Will, and Rolf Backofen. The energy landscape library - a platform for generic algorithms. In *Proc. of BIRD'07*, volume 217, pages 83–86. OCG, 2007.
- [12] Christoph Flamm, Ivo L. Hofacker, Sebastian Maurer-Stroh, Peter F. Stadler, and Martin Zehl. Design of multi-stable RNA molecules. *RNA*, 7:254–265, 2000.
- [13] Ken A. Dill. Theory for the folding and stability of globular proteins. *Biochemistry*, 24:1501–1509, 1985.
- [14] Martin Mann, Daniel Maticzka, Rhodri Saunders, and Rolf Backofen. Classifying protein-like sequences in arbitrary lattice protein models using LatPack. *HFSP Journal*, 2(6):396, 2008. Special issue on protein folding: experimental and theoretical approaches.
- [15] T. Wüst and D.P. Landau. The HP model of protein folding: A challenging testing ground for Wang-Landau sampling. *Computer Physics Communications*, 179(1-3):124–127, 2008. Special issue based on the Conference on Computational Physics 2007 - CCP 2007.
- [16] P. E. Leopold, M. Montal, and J. N. Onuchic. Protein folding funnels: kinetic pathways through a compact conformation space. *Proc. Natl. Acad. Sci. USA*, 89:8721–8725, 1992.
- [17] Konstantin Klemm, Christoph Flamm, and Peter F. Stadler. Funnels in energy landscapes. *The European Physical Journal B*, 63(3):387–391, 2008.
- [18] Michael R. Garey and David S. Johnson. *Computers and intractability*. Freeman, 1979.
- [19] Stephan Mertens. A physicist's approach to number partitioning. *Theor. Comp. Sci.*, 265(1-2):79–108, 2001.
- [20] Peter F. Stadler, Wim Hordijk, and José F. Fontanari. Phase transition and landscape statistics of the number partitioning problem. *Phys. Rev. E*, 67(5):056701, May 2003.
- [21] Fernando F. Ferreira and José F. Fontanari. Probabilistic analysis of the number partitioning problem. *Journal of Physics A: Mathematical and General*, 31(15):3417–3428, 1998.
- [22] Christoph Flamm, Walter Fontana, Ivo Hofacker, and Peter Schuster. RNA folding kinetics at elementary step resolution. *RNA*, 6:325–338, 2000.
- [23] Kay C. Wiese and Edward Glen. jViz.Rna - an interactive graphical tool for visualizing rna secondary structure including pseudoknots. *IEEE Symposium on Computer-Based Medical Systems*, 0:659–664, 2006.
- [24] Ivo L. Hofacker, Walter Fontana, Peter F. Stadler, L. Sebastian Bonhoeffer, Manfred Tacker, and Peter Schuster. Fast folding and comparison of RNA secondary structures. *Chemical Monthly*, 125:167–188, 1994.
- [25] I. Tinoco, O. C. Uhlenbeck, and M. D. Levine. Estimation of secondary structure in ribonucleic acids. *Nature*, 230:362–367, April 1971.
- [26] S. M. Freier, R. Kierzek, J. A. Jaeger, N. Sugimoto, M. H. Caruthers, T. Neilson, and D. H. Turner. Improved free-energy parameters for predictions of RNA duplex stability. *Proceedings of the National Academy of Sciences of the United States of America*, 83(24):9373–9377, 1986.
- [27] S. Kullback. The Kullback-Leibler distance. *The American Statistician*, 4:340–341, 1987.